Energy Equip. Sys. / Vol. 9/No. 1/March 2021/ 91-106

Energy Equipment and Systems

http://energyequipsys.ut.ac.ir
www.energyequipsys.com

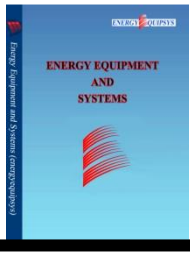

Optimization of vapor compression refrigeration cycle considering a binary mixture of working fluids using evolutionary algorithms

Authors

Hassan Hajabdollahi[a]
Mohammad Shafiey Dehaj[a*]

[a] Department of Mechanical Engineering, Vali-e-Asr University of Rafsanjan, Rafsanjan Iran

Article history:

Received : 5 May 2020
Accepted : 13 July 2020

ABSTRACT

The mixture of refrigerants including R32, R125, R134a, and R125 are applied in a vapor compression refrigeration cycle. Four design parameters are selected to optimize the total annual cost (TAC) and coefficient of performance (COP) in two steps. Firstly, the cycle is modeled by the mixture of R32 and R125, and secondly is done by a mixture of R134a and R125. It is revealed that COP and TAC are improved by an increase in the percent of R32. Moreover, COP and TAC are improved by an increase of R32 percentage. In the second step, the cycle has the highest COP and lowest TAC, where the pure R134a is applied, and the lowest COP is observed where the refrigerant is composed of 40% and 60% of R134a and R125, respectively. Finally, optimization is performed in the case of R410a (50% R32 and 50% R125), and the results are compared with the first step.

Keywords: Mixture Working Fluid; NSGA-II; Total Annual Cost; Coefficient of Performance.

1. Introduction

Refrigeration technology plays an important role in human production and life; it is widely used in daily lives, commerce, and industrial production [1]. The industry has nearly always enhanced its effectiveness of energy use over the previous years. In the nearby years, the energy effectiveness is theoretically the most significant and cost-effective procedure to decrease greenhouse gas productions from manufacturing [2]. The working fluids performance in an organic Rankine cycle-vapor compression refrigeration (ORC–VCR) integrated system is considerable [3].

For a refrigeration cycle, the mixture of working fluids significantly affects the system performance. Mixtures have confident benefits over separate mechanisms, and they have been exploited valuably [4]. The effects of working fluids such as LiBr–H2O and NH3–H2O on the performance and energy consumption were investigated in several papers. A complete review of working fluids was presented by Jian et al [5]. In the other research Paurine, et al. investigated a new LiBr–H2O vapor absorption refrigeration (VAR) system, to described the effects of the working fluids [6]. Kim et al. [7] using R32, R134a, R152a and R1234yf as the refrigerants studied the effectiveness of waste heat recovery systems of a marine gas turbine which included the Rankine cycle and the organic Rankine cycle to form a dual-loop cycle. The results showed that the All of the working fluids have better performance than for the single-loop cycle, and the maximum effectiveness with energy and exergy aspect of 29.50 % and 45.58 % related to the R134a. A Computer-Aided Molecular

* Corresponding author: Mohammad Shafiey Dehaj
Department of Mechanical Engineering, Vali-e-Asr University of Rafsanjan, Rafsanjan Iran
Email: m.shafiey@vru.ac.ir

Design (CAMD) procedure to choose the binary working fluid mixtures used in Organic Rankine Cycles (ORC) was done by Papadopoulos et al. [8]. The mixture of refrigerants as working fluid has been investigated by many refrigeration and heat pump cycle researchers. A new Rankine power cycle that used a mixture of three hydrocarbons as working fluid was suggested by Sun et al. to find a high efficiency [9]. She et al. provided a hybrid energy-efficient refrigeration system combined with LiCl, LiBr and CaCl2 aqueous solutions for an improvement of effectiveness [10]. During recent years many thermodynamic models were developed to improve the organic Rankine cycle/vapor compression cycle (ORC/VCC). Bu et al. investigated an ORC/VCC ice maker driven by solar energy, and different refrigerants such as R123, R245fa, R600a and R600 were chosen to recognize the high system efficiencies [11]. A cold room assisted vapor-compression refrigeration cycle is dynamically modeled in a year and optimized by Hajabdollahi and Hosseini [12]. The optimum solutions show that R407c is the best refrigerant in both thermodynamics and economics viewpoints with 9148.2 $/year as total annual cost and 6.12 for COP. Akbari et al. provided a novel comprehensive approach for the selection of the most appropriate working fluids and the conceptual design of vapor-compression refrigeration cycles, subject to minimal overall conductance for fixed cooling capacity with constant temperatures of the external fluids entering the condenser and the evaporator [13]. dos Santos Napoleao et al. calculated the entropy of ammonia-water mixture as a function of temperature, pressure, concentration, and other thermodynamic properties associated with the absorption process, to support energy and exergy analysis of absorption. refrigeration systems [14].

According to much research, it was found that the traditional working fluids have low-grade heat energy, and most of them have great global warming possibilities (GWP) or even are combustible or deadly. Therefore, to reduce the above difficulties, zeotropic mixtures of carbon dioxide in a transcritical Rankine cycle (TRC) were investigated by Dai et al. to improve thermal efficiency [15]. Modyi and Haghlind presented a review of the recent research on power cycles with zeotropic mixtures as the working fluid [16]. Andreasen et al. presented an assessment of procedures for estimating and comparing the thermodynamic performance of working fluids for organic Rankine cycle power systems [17].

To evaluate COP and cooling capacity, the main parameters of the ejector for an air-cooled ejector cycle using R134a were designed by Jia and Wenjian [18]. A new configuration of absorption refrigeration machine based on phase separation has been studied by Ouassila et al. to investigate the performance [19]. In another research, a novel ejector increased the operating of vapor compression refrigeration cycle with the mixtures of refrigerants R32 and R125 was investigated by Yu et al. for recovering the expansion process losses of the cycle [20]. They demonstrated that the established cycle gave a greater cooling (heating) capacity and a greater COP. This cycle contributed to the using R32 in air-conditioner systems as the refrigerant. To compare the performances for different mixtures, Yang et al. performed a study on a combined power and ejector refrigeration cycle using zeotropic mixture isobutane/pentane theoretically [21]. It should be mentioned that chlorofluorocarbon refrigerants have extremely adverse environmental effects since they deplete atmospheric ozone [22]. Zhao et al. also presented a novel optimization strategy for the vapor compression refrigeration cycle [23]. In another paper a model-based decentralized optimization procedure for vapor compression refrigeration cycle (VCC) was demonstrated by Zhao et al. They illustrated the acceptable precision of the prediction and influence of practical energy saving of the suggested technique [24].

Zhang et al. [25] evaluated and optimized the subcritical organic Rankine cycle to recover low-grade waste heat of flue gas were by the cost of the electricity generation. They founded that the finest temperatures of evaporating and condensing are essentially affected by the temperatures of inlet flue gas temperature and cooling fluid temperature, respectively. Moghimi et al. reported a comprehensive 4E analysis of a novel Combined Cooling, Heating, and Power cycle (CCHP). They used Thermo-economic Multi-objective optimization performed a parametric study and determined the influences of different design variables on the system performance [26]. Energy, exergy and economic analyses for a combined cycle power plant (CCPP) with a supplementary firing system were done by Khademi et al. [27]. Hajabdollahi and Esmaieli studied a regenerative organic Rankine cycle (RORC) and optimized it for using waste heat recovery from a prime mover [28]. The results in the case of a diesel engine working with R123 indicated a 2% and 2.52% enhancement in the performance and the total annual cost, respectively, in comparison to the case of a gas engine working with R123. Salim et al. performed the multi-objective optimization of a combined power (organic Rankine cycle) and vapor compression refrigeration cycle based on heat source temperatures ranging from 120 °C to 150 °C. The optimal system with R245fa indicated the best performance based on both objective functions [29]. Petrovic et al. proposed a multi-objective optimization of a geothermal water desalination plant with an ejector refrigeration system. They performed sensitivity analysis and obtained Optimal design point and refrigerant by decision-making analysis [30].

Refrigeration system combined by other technology to improve performance has improved significantly in the recent years. A combined-cycle has been proposed by Abed et al. for the production of power and refrigeration simultaneously [31]. They carried out the optimization by choosing the inlet pressure of the turbine, temperature of superheated vapor and temperature of the condenser as design parameters. Kaska analyzed the performance of the combined cooling cycle with the Organic Rankine power cycle. They calculated the efficiency coefficient of the total system based on varying pre-cooling values. Results determined that cold entry of hydrogen into the Claude cycle reduced the energy consumption needed for liquefaction [32]. Ma et al. suggested a novel closed Brayton cycle using supercritical CO_2–Kr mixture as working fluid integrated with an absorption chiller (CBC/AC). They optimized the main variables by considering varied T_0 working conditions. The results showed that the energy and exergy performance of the CBC/AC are enhanced relative to the S-CO_2 cycle [33].

The above review of the available literature indicated that the considerations strictly have been focused on the thermo-economic optimization of vapor with binary mixture working fluids. since the Mixtures of working fluid have certain advantages over individual components, and these have been exploited advantageously [4 and 8]. Furthermore. uncertainty in the context of mixture design and selection is an additional important issue that deserves attention. As a result, in this paper, a vapor compression refrigeration cycle is considered, using the mixtures of working fluids including R32, R125, R134a and R125 to improve COP and TAC. On the other hand, the fast and elitism non dominated sorting genetic algorithm (NSGA-II) is employed to maximize the COP and minimize the TAC simultaneously. Also to consider the optimum amounts of COP and TAC the multi-objective optimization should be applied in this problem. For this reason, four design parameters are selected to optimize the two objective functions in two steps. Firstly, the system is designed by a mixture of R32 and R125, and secondly is performed by a mixture of R134a and R125. Finally, optimization is performed in the case of R410a (50% R32 and 50% R125), and the results are compared with the first step. Finally, optimization is carried out in the case of R410a (50% R32 and 50% R125), and the results are compared with the first step.

Nomenclature

A	heat transfer surface area (m^2)
C	investment cost ($)
C_v	expansion valve coefficient
COP	coefficient of performance (-)
h	enthalpy (kJ kg-1 k-1)
$\dot{H}$	rate of heat (kW)
i	interest rate (-)
LHV	fuel lower heating value (kJ kg-1)
$\dot{m}$	mass flow rate (kgs^{-1})
p	pressure (kPa)
r_p	compressor pressure ratio (-)
TAC	total annual cost ($/year)
T	temperature (°C)

U	overall heat transfer coefficient (W/m^2. K)
$\dot{W}$	power (kW)
y	depreciation time (year)

Greek symbols

α	annual cost coefficient (-)
ψ_{el}	electricity unit cost ($/kWh)
τ	the step size of variation in loads during a year (month)
Δp	pressure drop (kPa)
ρ	density (kg /m^3)
η	efficiency (-)

Subscripts

a	actual
amb	ambient
comp	compressor
cond	condenser
exp	expansion
evap	evaporator
i	inlet
inv	investment
o	outlet
op	operational
r	refrigerant
s	isentropic
v	valve

2. Thermal Modeling

Because of very expensive tests in the experimental analysis of energy systems (especially optimal design of these systems), it is reasonable to find the optimal design in the numerical or analytical method. So, numerical analysis is selected in this paper to model the refrigeration cycle. For this purpose, well-known models based on the first law of thermodynamic, the second law of thermodynamic, and heat transfer relations for each equipment are selected. The refrigeration cycle diagram will always have the same basic components. These components may be in different shapes, capacity and sizes, but they all do the same thing. In the refrigeration cycles, an expansion valve, a compressor, condenser and evaporator are applied (Fig. 1 illustrates the schematic diagram of this system). In the present cycle, R32 vapor or R125 vapor as the circulating refrigerant goes in the compressor (in state 1). In the compressor, it is compressed at the isentropic process and leaves the compressor as superheated vapor (in state 2). After that, it passes among the condenser which first makes cold and eliminates the superheat and then condenses the vapor and converts it into a liquid with the loss of excess heat in the fixed temperature and pressure (in state 3). The liquid arrives at the expansion valve where its pressure suddenly reduces (in state 4). That produces a mixture of liquid - vapor at a lower pressure and temperature. Accordingly, the mixture goes through the tubes of the evaporator and is entirely vaporized by absorbing the heat of hot air. Finally, the resulted vapor comes back to the inlet of the compressor, and thus the thermodynamic cycle is completed. A simulation model is expanded to find the COP of the refrigeration by considering the under assumptions:

1. The process is supposed to be steady-state.
2. The expansion process of the refrigerant liquid is regarded to be isentropic.
3. Pressure drop in the evaporator and condenser is assumed to be 5%.

The thermodynamic equations for different components of the present system are illustrated in Fig. 1.

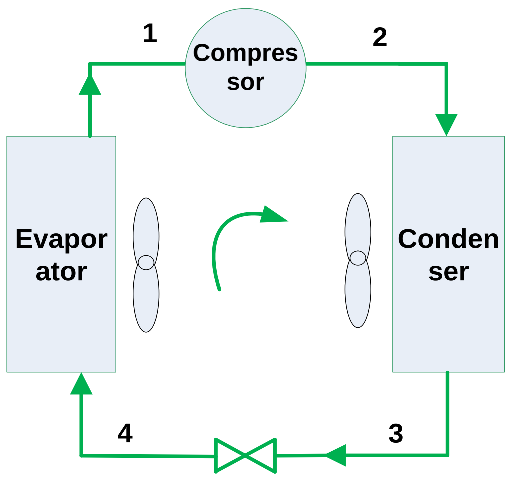

Fig. 1. Schematic diagram of heat pump system

2. 1. Compressor

The compressor is considered the heart of the refrigeration cycle. It's one of the divided points between high and low sides. Its function is to pump the vapor from the evaporator, enhances its pressure, and send the high-pressure vapor to the condenser. The compressor isentropic efficiency is the ratio of ideal (isentropic) to the real needed power as given by [34]

$$\eta_{comp} = \frac{\dot{W}_{comp,s}}{\dot{W}_{comp}} = \frac{h_1 - h_{2,s}}{h_1 - h_2} \quad , \tag{1}$$

where h is the specific enthalpy of refrigerant, and subscripts 1, 2 and s represent the inlet of the compressor, the outlet of the compressor, and the isentropic compression process, respectively. Moreover, the isentropic efficiency of the compressor is related to the pressure ratio (r_p) and can be evaluated by [35]

$$\eta_{comp} = C_1 - C_2 * (r_p) \quad , \tag{2}$$

where r_p presents the pressure ratio defined as P_2 / P_1.

The compressor work is given by

$$\dot{W}_{AC} = \dot{m}_a . C_{p,a} (T_2 - T_1) \quad . \tag{3}$$

2. 2. Condenser and evaporator

A condenser acts the same way as the evaporator but it works the opposite. In the condenser, heat is taken from the flowing fluid, and then condenses and converts a liquid at high pressure. Therefore, by considering the energy balance for refrigerant and air

$$\dot{H}_{cond} = \dot{m}_{ref} (h_2 - h_3) = \dot{m}_{air} c_{p.air} \Delta T_{air} = UA_{cond} \Delta T_{LMTD,cond} \quad , \tag{4}$$

where ΔT_{air},U, and A_c are air temperature difference, coefficient of the total heat transfer, the surface area of condenser, respectively. $\Delta T_{LMTD,c}$ is logarithmic mean temperature difference defined as

$$\Delta T_{LMTD,cond} = \frac{\Delta T_1 - \Delta T_2}{\log(\Delta T_1 / \Delta T_2)} = \frac{(T_2 - T_{air,out}) - (T_3 - T_{air,in})}{\log((T_2 - T_{air,out})/(T_3 - T_{air,in}))} \quad . \tag{5}$$

The condenser pressure drop (ΔT_{cond}) is calculated from

$$\Delta p_{cond} = 1 - p_3 / p_2 \quad . \tag{6}$$

As was mentioned above the thermal modeling of the evaporator is the same as the condenser.

2. 3. Expansion valve

All expansion components to some extent have a similar function. It controls to provide the correct amount of refrigerant flow into the evaporator. The mass flow rate through the valve is estimated using

$$\dot{m}_r = C_v \sqrt{\rho_{v,i} \Delta p_v} \quad . \tag{7}$$

In the above equation, $C_v$is the coefficient of the expansion valve and the function of the opening degree of the valve. It is noticed that when the valve is fully open, C_v reaches the maximum value.

3. Objective functions, design parameters and constraints

To optimize the various objectives simultaneously, the multi-objective optimization procedure is used. A multi-objective problem consists of optimizing (i.e., minimizing or maximizing) several objectives simultaneously, with a number of inequality or equality constraints [36]. Accordingly, the optimum Pareto front which is a set of non-dominated points is acquired. In the present research, the fast and elitism non dominated sorting genetic algorithm (NSGA-II) is employed to maximize the COP and minimize the TAC simultaneously. In the all studied cases, a population size of 200 chromosomes has been selected with a crossover probability of 0.8, mutation probability of 0.02 and an elitism parameter of 0.55. The influence of elitism is provided by selecting the number of individuals from each subpopulation, based on the [37]

$$S_q = S \frac{1-c}{1-c^w} c^{q-1}. \tag{8}$$

To create a parent search population, P_{t+1} (t indicates the generation), S demonstrates the size where $0 < c < 1$, and w presents the overall number of ranked non-dominated.

3.1. Crowding distance

In the present work, the crowding distance metric suggested by Deb [38] is applied. An individual crowding distance is the perimeter of a rectangle with its nearest neighbors at diagonally opposite corners. Therefore, when individual $X^{(a)}$ and individual $X^{(b)}$ have an equal rank, it can be said that the individual with a bigger crowding distance is better.

3.2. Crossover and mutation

To find the offspring population, Q_{t+1} random unvarying mutation and constant crossover are utilized. The integer-based uniform crossover operator takes two distinct parent individuals and interchanges each corresponding binary bit with a possibility, $0 < p_c \leq 1$ [39]. Resulting crossover, the mutation operator varies each of the binary bits with a possibility, $0 < P_m < 0.5$. As mentioned above, optimization is performed by regarding the COP and TAC as objective functions. The TAC includes the cost of investment (the capital price of components of the system) and the working price of the compressor. Thus,

$$C_{total} = \alpha C_{inv} + C_{op} \quad , \tag{9}$$

$$\begin{aligned} C_{inv} &= C_{inv,cond} + C_{inv,evap} + C_{inv,comp} + C_{inv,\exp} \\ &= b_1 (A_{cond})^{d_1} + b_2 (A_{evap})^{d_2} + b_3 (\dot{W}_{comp})^{d_3} + b_4 (\dot{m}_r)^{d_4} \end{aligned} \tag{10}$$

$$C_{op} = C_{op,comp} = \sum_{i=1}^{i=N} \left(\psi_{el} \times \dot{W}_{comp,i} \right) \times \tau_i \quad , \tag{11}$$

where the b and d are constant coefficients and their values related to the local price of the equipment. Also, τ_i and N are the step size of changing of request capacity in a year (month) and month number during a year, respectively. Besides, α is the coefficient of the TAC which is given by

$$\alpha = \frac{i}{1-(1+i)^{-y}} \quad , \tag{12}$$

in which i and y are the rate of interest and reduction time, respectively. The thermal performance of a heat pump system is given by a parameter named the COP which is given by

$$COP = \frac{\sum_{i=1}^{N} \dot{H}_{cond,i} \times \tau_i}{\sum_{i=1}^{N} \left(\dot{W}_{comp,i} + \dot{m}_{fuel,i} \times LHV \right) \times \tau_i} \quad . \tag{13}$$

Furthermore, design parameters are evaporator pressure, condenser pressure, and the value of superheating/subcooling in evaporator/condenser. The constraints are considered to be as follows:

$$P_2 < 2000 \tag{14}$$

$$T_4 \leq 5 \tag{15}$$

$$T_2 > 50 \tag{16}$$

This constraint, $T_2 > 50$, is necessary to keep the temperature of the condenser above the outdoor temperature for condensing to be possible.

4. Case study

In the present research, the mixtures of refrigerants involving R32, R125, R134a and R125 are applied in a vapor compression refrigeration cycle. Also, hot stream of oil with a mass flow rate of 8kg/s and temperature of the inlet at 78.3 °C, which is cooled by liquid water with an inlet temperature of 30 °C. Additionally, Al_2O_3 is chosen as a nanoparticle in the pipe side of the STHE. For modeling of the system, input parameters are defined in the Table. 1. Thermophysical properties of two streams are related to the temperature and calculated based on the average temperature of the inlet and outlet. Moreover, density of Al_2O_3 is 3950 kg/m^3 [38].

Table. 1. Design parameters and their range of variations

	Lower bound	**Upper bound**
Evaporator pressure (kPa)	5	1000
Compressor pressure ratio (-)	1.1	5
Value of superheating in the evaporator (°C)	0	20
Value of sub-cooling in condenser (°C)	0	20

The refrigeration cycle must provide 100 kW output net power to operate at $\tau = 5000$ hours in a year. The optimization is carried out for interest rate 0.1 and for depreciation time 15 years. In this study, 5% are assumed for the pressure drop in the evaporator and condenser. In addition, the constants in Eq. (10) are assumed b = [748 499 233 400] and d = [0.16 0.16 0.95 1].

5. Results and discussion

5. 1. Optimization result for the mixture of R125 and R32

To optimize COP and TAC as objective functions, four design parameters including evaporator pressure, compressor pressure ratio,the value of superheating in the evaporator, and the value of sub-cooling in the condenser are considered as the variables. The variations of four design parameters are provided in the Table. 1. The refrigerants are applied in the cycle as the working fluids are applied in two steps. Firstly, the refrigeration cycle is modeled by the mixture of R32 and R125 and is subsequently analyzed by the mixture of R134a and R125 whose percentages are illustrated in six cases in Tables 2 and 3, separately. Finally, the cycle is modeled by applying R410a as the working fluid which its chemical formula is the mixture of 50% R32 and 50% R125. As it can be seen in Table 2 case 1 and case 2 are pure R125 and R32, respectively. Design parameters values and objective functions for the final optimum point in the different studied cases are brought in Tables 4 and 5. Objective functions involving COP and the TAC obtained in the final optimum point are demonstrated in Table.4 for six investigated cases itemized in Table 2. The refrigeration cycle in case 6 has the highest COP as compared with other studied cases, where the pure R32 is applied as the working fluid. It is noted that COP is improved by an increase in the percent of R32. On the other hand, the lowest COP is observed in case 1 where the working fluid is pure R125. The lowest total annual cost happens in case 6 where the pure R32 is used as the working fluid and the TAC increases by a decrease in the fraction of R32. On the other hand, the highest TAC is achieved in case 1 where the working fluid is composed of pure R125. Optimization objective functions have been fitted using

$$COP(-) = 2.077\times10^{-7}(m_f)^4 - 3.032\times10^{-5}(m_f)^3 + 9.286\times10^{-4}(m_f)^2 + 0.04056(m_f) + 5.202 \quad (17)$$

$$TAC(\$/year) = -1.325\times10^{-4}(m_f)^4 + 0.0144(m_f)^3 + 0.38(m_f)^2 - 92.98(m_f) + 10640.1 \quad (18)$$

Table. 2. Different studied cases in the first case study

	Percent of R32 (%)	Percent of R125 (%)
Case 1	0	100
Case 2	20	80
Case 3	40	60
Case 4	60	40
Case 5	80	20
Case 6	100	0

Table. 3. Different studied refrigerant fraction in the second case study

	Percent of R134a (%)	Percent of R125 (%)
Case 1	0	100
Case 2	20	80
Case 3	40	60
Case 4	60	40
Case 5	80	20
Case 6	100	0

Table. 4. Values of design parameters and objective functions for the final optimum point in the cases listed in Table. 2

	Case 1	Case 2	Case 3	Case 4	Case 5	Case 6
Evaporator pressure (kPa)	642.57	829.30	762.48	762.49	850.13	859.37
Compressor pressure ratio (-)	2.61	2.31	2.13	2.07	2.07	1.83
Value of superheating (°C)	11.25	5.00	10.00	7.50	0.62	5.00
Value of sub-cooling (°C)	10.62	11.25	2.91	1.00	4.68	0.46
COP (-)	5.1959	6.2044	6.8422	7.1798	7.3445	9.0023
Total annual cost ($/year)	10645.0	9001.6	8161.1	7773.2	7605.4	6290.0

Table. 5. Values of design parameters and objective functions for the final optimum point for the cases listed in Table. 3

	Case 1	Case 2	Case 3	Case 4	Case 5	Case 6
Evaporator pressure (kPa)	642.57	628.90	540.11	473.31	395.81	316.29
Compressor pressure ratio (-)	2.61	2.56	3.05	3.05	2.59	2.56
Value of superheating (°C)	11.25	4.63	0	0	3.83	7.74
Value of sub-cooling (°C)	10.62	13.74	19.86	19.87	12.45	9.92
COP (-)	5.1959	5.6893	4.8676	5.0405	6.2218	6.4360
Total annual cost ($/year)	10645.0	9780.9	11307.8	10954.3	8980.3	8696.5

to find the exact information in the final points. In the above equation m_f demonstrates the R32 mass fraction in the refrigerant mixture which varies between 0 to 100 percent. The function error for the equations represented above is less than 1%. The optimum Pareto fronts of TAC versus COP for these six mixtures are illustrated in Fig. 2. In case 1 where the refrigerant is R125, TAC is approximately achieved 11000 for the COP around 5.2. For the COP of around 6.2, this figure decreases to 9000 where the mixture is included 20% R32 and 80% R125. This trend continues in the four other cases. In fact, by an increase in the percentage of R32, objective functions tend to be much more optimized. This concept is also derived from Fig. 3 in which case 6 has the best result as well as COP and TAC are 7.4 and 7500 dollars per year, respectively. Finally, it is recognized that case 5, case 4, case3, case 2 and case 1 are in the next ranking, respectively.

The Pareto optimum results shown in Fig.3 reveal that there is no conflict among both objectives, the COP and TAC. Any change that improves the COP, does not lead to a significant variation in the TAC and vice versa. It is detected that the finest refrigerant for this case study is R32 since their results perfectly indicate over the other mixed refrigerants and R125 in both COP and TAC. Optimum values of design parameters for different studied cases are illustrated in Fig. 4. Evaporator pressure for six types of mixtures was shown in Fig. 4. A. Evaporator pressure is reduced by a decrease of R32 in the mixture, and this trend continues in the diagram. There is an exception in which case 2 needs higher evaporator pressure than cases 3 and 4. It is worth mentioning that in cases 3 and 4 equal evaporator pressure is needed for multi-objective optimization. For the compressor pressure ratio, the trend is quite regular and the opposite of the evaporator pressure trend (as illustrated in Fig. 4.b). An enhance in the percent of R32 reduces the pressure ratio in the optimum points and this situation continues for all studied cases. By increase of R32 in all mixtures except for the case 2 and 6, Value of superheating in evaporator decreases in optimum points (as shown in Fig. 4. c). It is demonstrated that there is no regular trend in the values of sub-cooling in the condenser in the optimized point for all cases while maximum and minimum sub-cooling happen in the case 2 and 6, respectively (Fig. 4. d).

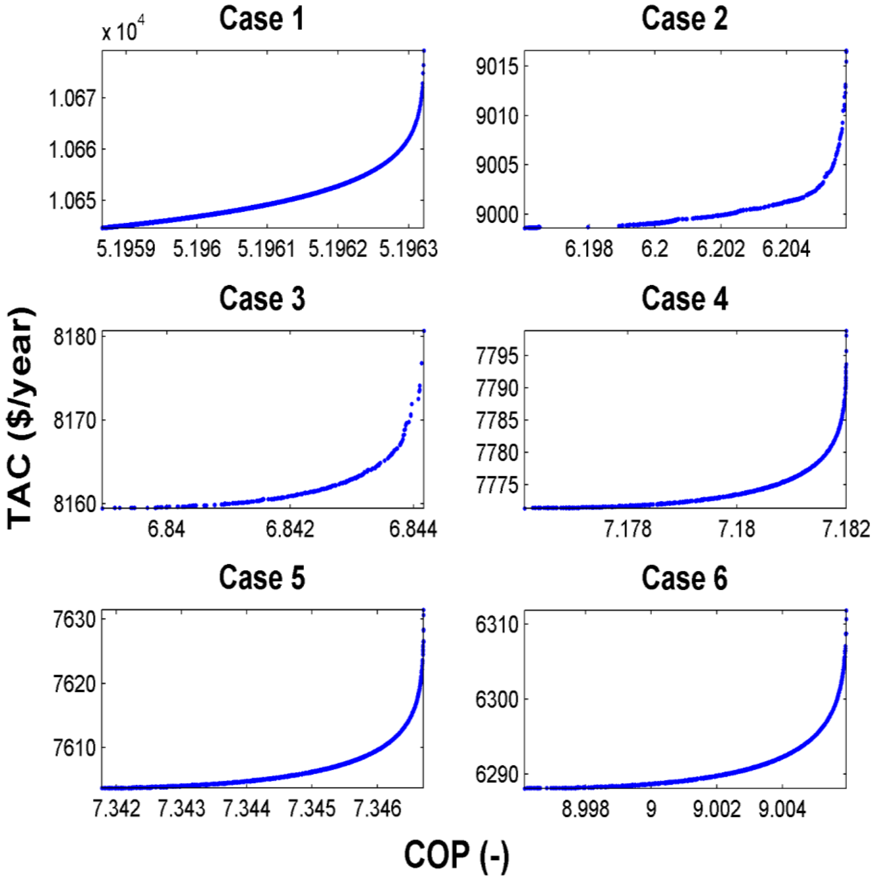

Fig. 2. Optimum Pareto fronts for a different mixture between R32 and R125

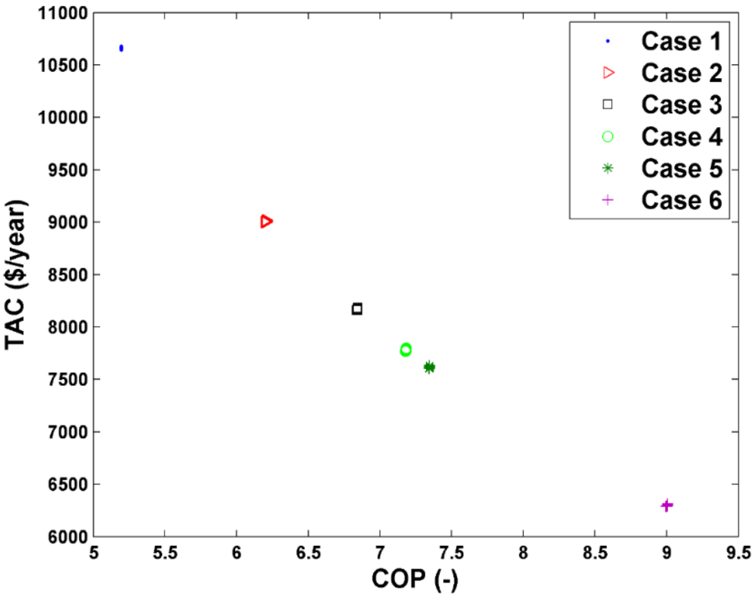

Fig. 3. Optimum Pareto fronts for a different mixture between R32 and R125 in a figure

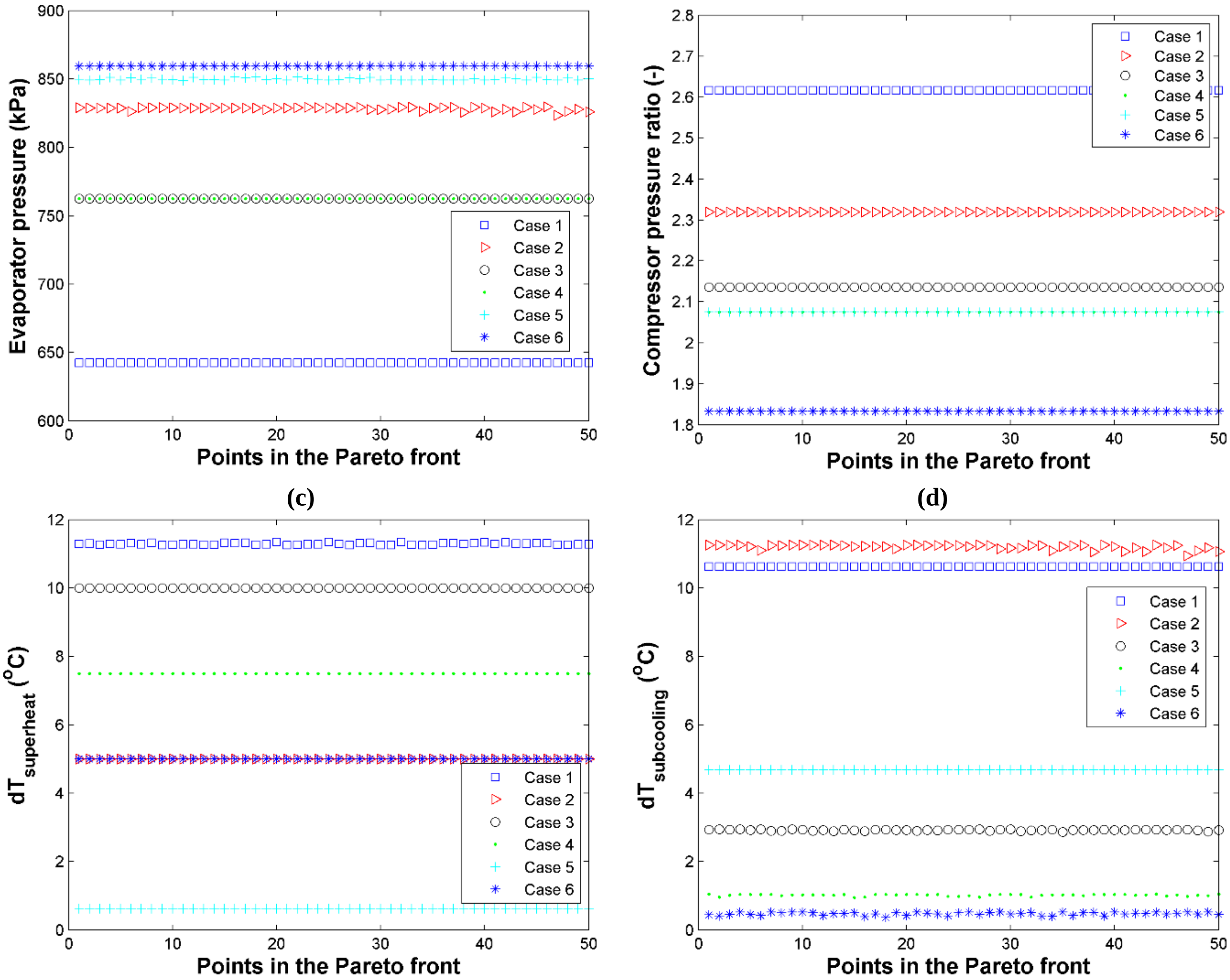

Fig. 4. Optimum values of design parameters for different studied cases

5. 2. Optimization result for the mixture of R125 and R134a

In the second case study, a different fraction of studied refrigerant is listed in Table 3, where the mixture of R134a and R125 is used as the working fluid. Case 1 and case 6 are assumed to be pure R125 and R134a, respectively, and four other cases show the different fractions for the mixtures of R134a and R125. Objective functions including COP and the TAC obtained in the final optimum point are demonstrated in Table. 5 for six studied cases provided in Table. 3. Refrigeration cycle in case 6 has the highest COP as compared with other studied cases, where the pure R134a is applied as the working fluid, and case 5, case 2, case1, and case 4 are located in the next ranking. On the other hand, the lowest COP is observed in case 3 where the working fluid is composed of 40% and 60% of R134a and R125, respectively. The lowest total annual cost happens in case 6 where the pure R134a is used as the working fluid, and case 5, case 2, case 1 and case 4 are located in the next ranking. On the other hand, the highest TAC is achieved in case 3 where the working fluid is composed of 40% and 60% of R134a and R125, respectively. The total annual cost versus COP is depicted in the optimum Pareto fronts for different mixture in Fig. 5. It is deduced from these diagrams that there is no conflict between the total annual cost and COP. In other words, it can be said there is no significant variation in the TAC by an increase of COP. This concept is also understandable in which optimum Pareto

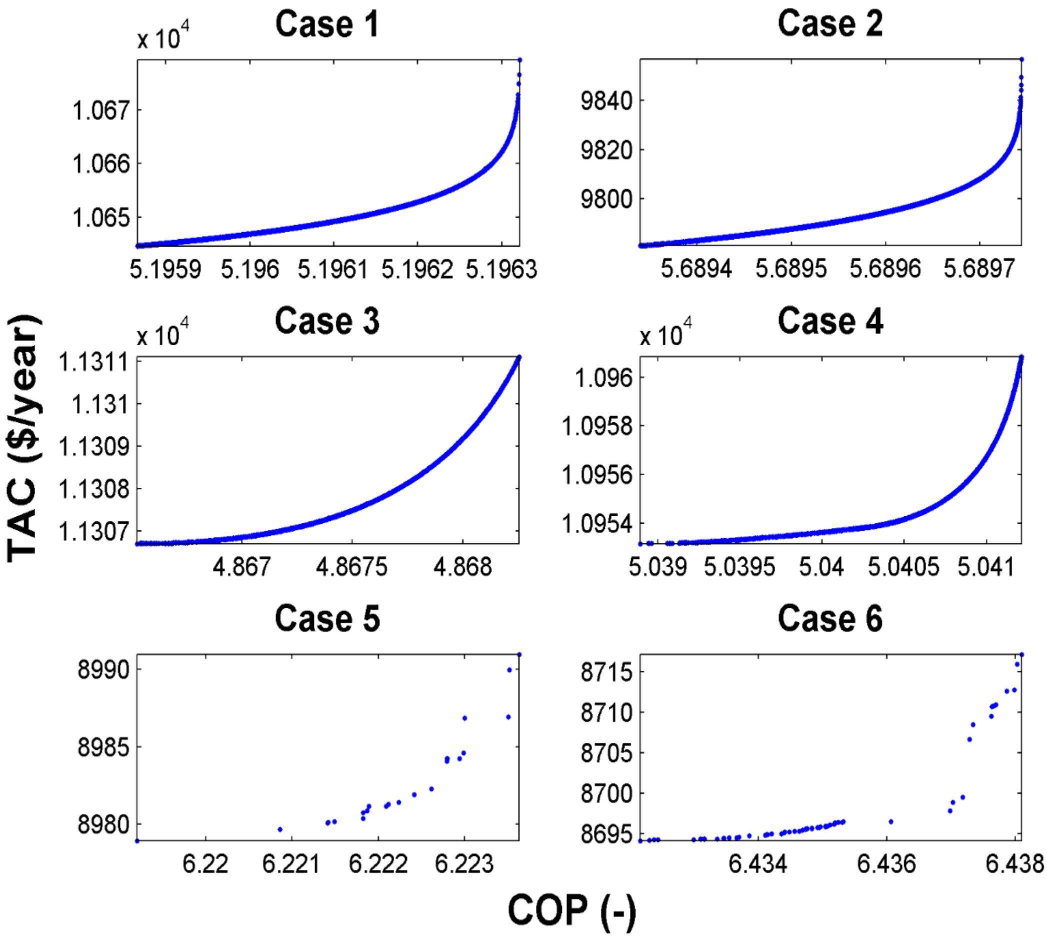

Fig. 5. Optimum Pareto fronts for a different mixture between R134a and R125

fronts for different mixtures are illustrated together in Fig. 6. It can be concluded that the best working fluid for the second case study is R134a since their results are perfectly indicated over the other mixed refrigerants in both COP and TAC. Optimum values of design parameters involving evaporator pressure, compressor pressure, superheat, and sub-cooling value for different studied cases are depicted in Fig. 7. Variation for all studied cases in evaporator pressure shows a regular trend, therefore by an increase in the percent of R134a evaporator pressure decreases. On the other hand, an evaporator with higher pressure is needed to optimize the refrigeration cycle by using R125. In the case of the compressor, the highest pressure is used when the composition of R125 and R134a is 60% and 40 % and vice versa. Using case 2 and case 6 provides the lowest pressure for the compressor and case 5 and case 1 are in the next ranking. The amount of superheating in case 1 is highest where the working fluid is just pure R125. Value of superheat decreases in case 6 and case 2 and 5 are in the next ranking as well as case 3 and 4 have the lowest amount of superheating. Such as superheating, the value of sub-cooling in the case 3 and 4 is the same and decreases in the case 2, 5, and 1, respectively. Finally, it should be mentioned that pure R134a presents the lowest amount of sub-cooling.

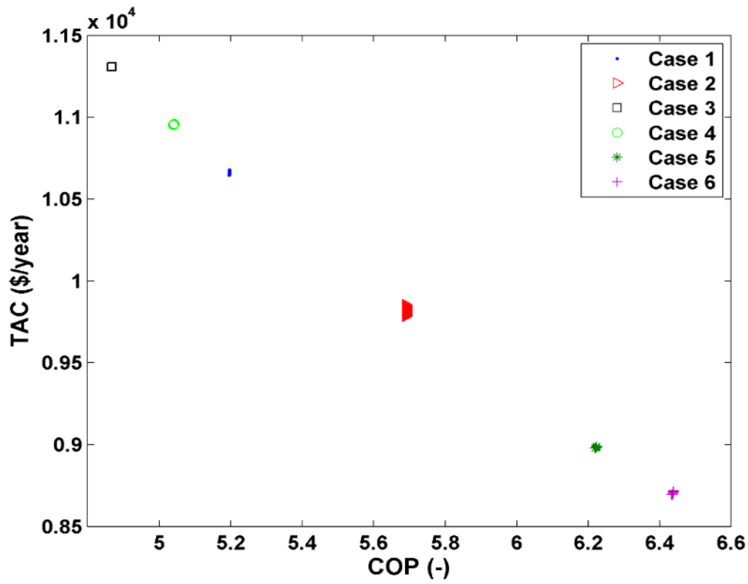

Fig. 6. Optimum Pareto fronts for a different mixture between R134a and R125 in a figure

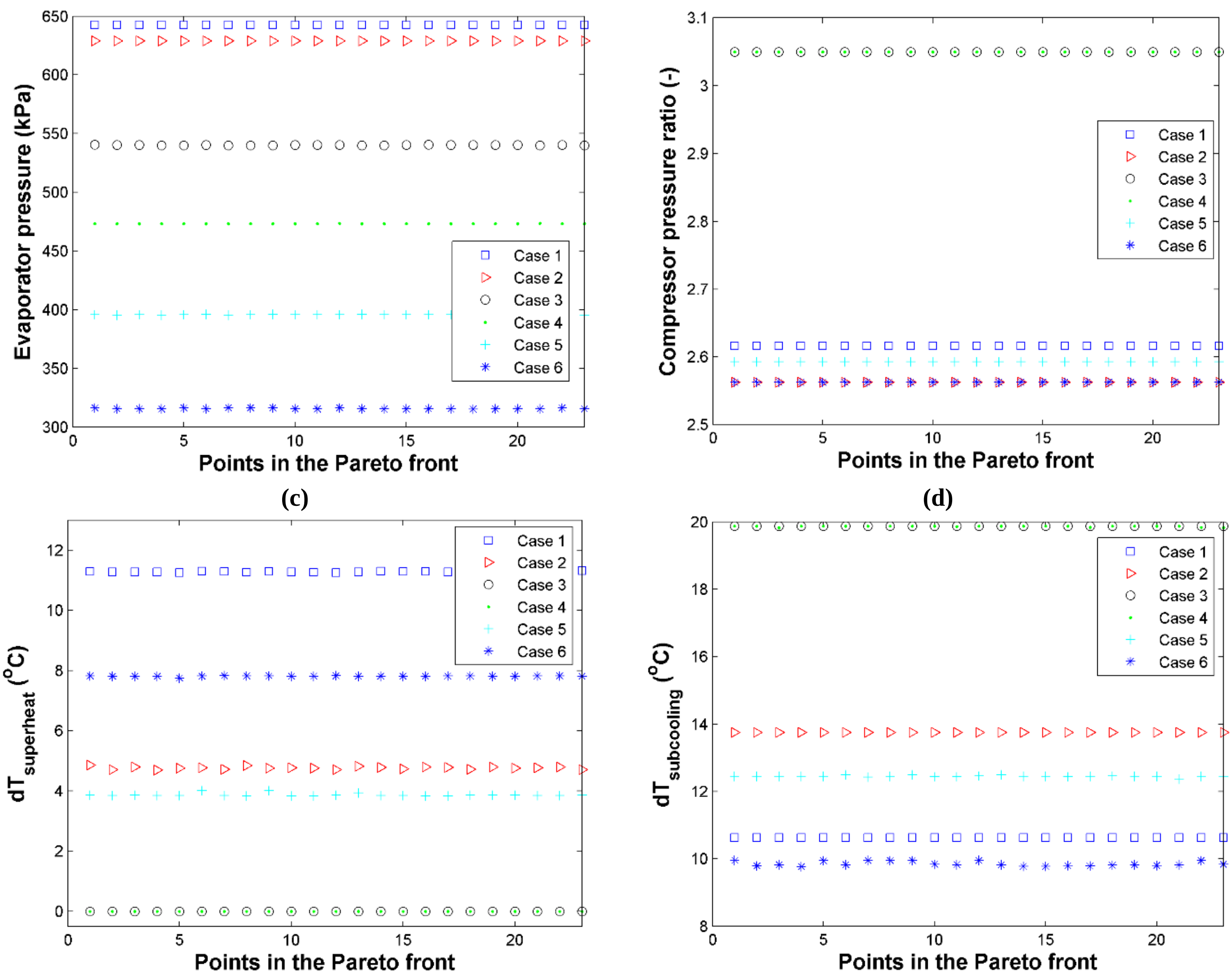

Fig. 7. Optimum values of design parameters for different studied cases

5. 3. Optimization result for the R410a

Optimum Pareto front in the case of R410a which its composition is R32 and R125 (50 and 50) is graphed in Fig. 8. Such as other refrigerants applied in the cycle, COP increases by the increase of TAC. Since we have the values of COP and TAC for case 3 and case 4 in the mixture of R125 and R132, therefore by interpolation method COP and its corresponding TAC can be obtained when the composition of both refrigerants is 50-50%. In fact, COP and its corresponding TAC are estimated to be 7.011 and 7967.15, respectively by interpolation. The COP in the case of R410a refrigerant is archived to be 7817.5, which the difference is 1.91%.

The optimal values of design parameters in the case of R410a are illustrated in Fig. 9 and the evaporator pressure and compressor pressure ratio are approximately 762 kPa and 2.1, respectively in the case R410a. These figures for the case 3 and 4 depicted in Fig. 4 are 760 kPa and 2.1(average of evaporator pressure and compressor pressure ratio in cases of 3 and 4), respectively.

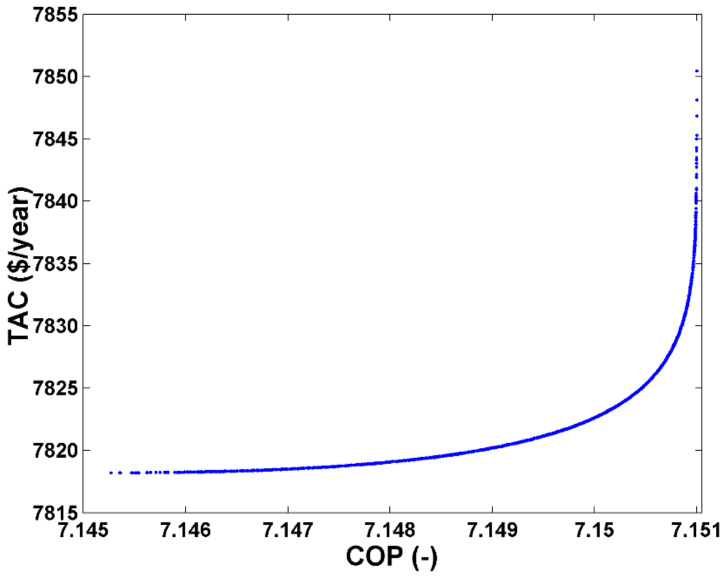

Fig. 8. Optimum Pareto front in the case of R410a

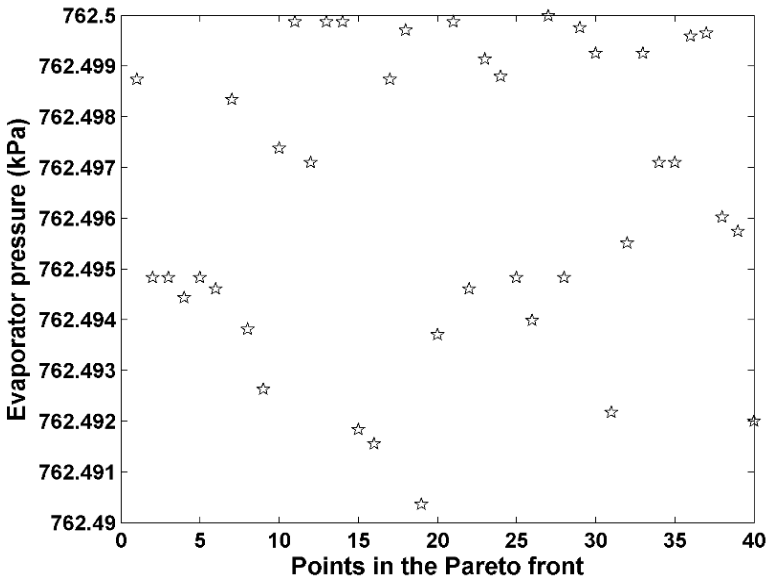

(b)

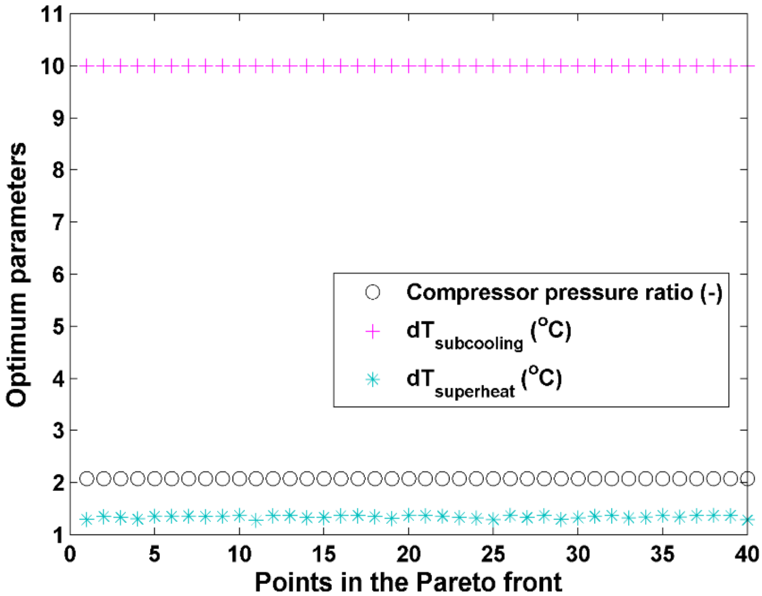

Fig. 9. Optimum values of design parameters in the case of R410a

6. Conclusion

Thermo-economic optimization of a vapor compression refrigeration cycle was performed by the NSGA-II method to maximize the COP and minimize the TAC. Four design parameters involving evaporator pressure, compressor pressure ratio, the value of superheating in the evaporator, and the value of sub-cooling in the condenser were selected. The working fluids of the cycle were applied in two steps. Firstly, the refrigeration cycle was modeled by the mixture of R32 and R125, and secondly was performed by the mixture of R134a and R125, and finally, optimization is done in the case of R410a which its composition is R32 and R125 (50% and 50%). The results show that the refrigeration cycle had the highest COP and lowest TAC when the pure R32 was applied as the working fluid. The lowest COP and highest TAC were observed where the working fluid was pure R125. In the second step, the highest COP and lowest TAC happened in the case of pure R134a, and the lowest COP was observed when the working fluid was included of 40% and 60% of R134a and R125, respectively. The best working fluid for the second studied case was obtained to be R134a. The results indicate that an increase in the percent of R134a led to a decrease in the evaporator pressure. On the other hand, an evaporator with a higher pressure was needed to optimize the refrigeration cycle by using R125.

References

[1] Pan, M., Zhao, H., Liang, D., Zhu, Y., Liang, Y., & Bao, G. (2020). A Review of the Cascade Refrigeration System. Energies, 13(9), 2254.

[2] Worrell, E., Bernstein, L., Roy, J. et al. Industrial energy efficiency and climate change mitigation. Energy Efficiency 2, 109 (2009).

[3] Saleh, B., Aly, A. A., Alogla, A. F., Aljuaid, A. M., Alharthi, M. M., Ahmed, K. I., & Hamed, Y. S. (2019). Performance investigation of organic Rankine-vapor compression refrigeration integrated system activated by renewable energy. Mechanics & Industry, 20(2), 206.

[4] Churi N, Achenie LE. "The optimal design of refrigerant mixtures for a two-evaporator refrigeration system." Computers & chemical engineering 21 (1997): S349-S354.

[5] J. Sun, L. Fu, S. Zhang, A review of working fluids of absorption cycles, Renewable and Sustainable Energy Reviews, 2012:16, 1899-1906.

[6] A. Paurine, G.G. Maidment, I.W. Eames, J.F. Missenden, Development of a thermo-gravity pumping mechanism for circulating the working fluids in a novel LiBr–H2O vapour absorption refrigeration (VAR) system, Applied Thermal Engineering, 5 December 2012:47, 25-33.

[7] Kim, J., Kim, D. & Kim, Y. Thermodynamic analysis of a dual loop cycle coupled with a marine gas turbine for waste heat recovery system using low global warming potential working fluids. J Mech Sci Technol 33, 3531–3541 (2019).

[8] A. I. Papadopoulos, M. Stijepovic, P. Linke, P. Seferlis, S. Voutetakis, Molecular Design of Working Fluid Mixtures for Organic Rankine Cycles, Computer-Aided Chemical Engineering, 2013:32, 289-294.

[9] H. Sun, H. Zhu, F. Liu, H. Ding, Simulation and optimization of a novel Rankine power cycle for recovering cold energy from liquefied natural gas using a mixed working fluid, Energy, 2014:70, 317-324.

[10] X.She, Y. Yin, X. Zhang, Suggested solution concentration for an energy-efficient refrigeration system combined with condensation heat-driven liquid desiccant cycle, Renewable Energy, 2015:83, 553-564.

[11] X.B. Bu, H.S. Li, L.B. Wang, Performance analysis and working fluids selection of solar-powered organic Rankine-vapor compression ice maker, Solar Energy,2013:95, 271-278.

[12] Hajabdollahi, H., & Hosseini, Z. (2020). Dynamical modeling and thermo-economic optimization of a cold room assisted vapor-compression refrigeration cycle. Energy Equipment and Systems, 8(2), 153-167.

[13] Akbari, H., Sorin, M., & Marcos, B. (2018). An equivalent temperature-based approach for selection of the most appropriate working fluids for refrigeration cycles. Energy Conversion and Management, 174, 227-238.

[14] dos Santos Napoleao, D. A., Silveira, J. L., Giacaglia, G. E. O., de Queiroz Lamas, W., & Araujo, F. H. M. (2017). Diagrams of entropy for ammonia-water mixtures: Applications to absorption refrigeration systems. International Journal of Refrigeration, 82, 335-347

[15] B. Dai, M. Li, Y. Ma, Thermodynamic analysis of carbon dioxide blends with low GWP (global warming potential) working fluids-based transcritical Rankine cycles for low-grade heat energy recovery, Energy,2014:64, 942-952.

[16] Modi, A., & Haglind, F. (2017). A review of recent research on the use of zeotropic mixtures in power generation systems. Energy Conversion and Management, 138, 603-626.

[17] Andreasen, J. G., Kærn, M. R., & Haglind, F. (2019). Assessment of methods for performance comparison of pure and zeotropic working fluids for organic Rankine cycle power systems. Energies, 12(9), 1783.

[18] Y.Jia, C. Wenjian, Area ratio effects to the performance of air-cooled ejector refrigeration cycle with R134a refrigerant, Energy Conversion and Management, 2012:53, 240-246.

[19] L. Ouassila, M. Abedeslam Hassan, Z. Ahmed, K. Yacine, C. Thierry, Study of New Absorption Refrigeration Cycle Operating with Partially Miscible Fluids Pairs, Energy Procedia, 2012:18, 1013-1022.

[20] J. Yu, X. Song, M. Ma, Theoretical study on a novel R32 refrigeration cycle with a two-stage suction ejector, International Journal of Refrigeration, 2013:36, 166-172.

[21] X. Yang, L. Zhao, H. Li, Z. Yu, Theoretical analysis of a combined power and ejector refrigeration cycle using a zeotropic mixture, Applied Energy, In Press, Corrected Proof, Available online 16 May 2015.

[22] Duvedi A, Achenie LE. "On the design of environmentally benign refrigerant mixtures: a mathematical programming approach."Computers & chemical engineering 21, no. 8 (1997): 915-923.

[23] L. Zhao, W. Cai, X. Ding, W. Chang, Model-based optimization for vapor compression refrigeration cycle, Energy, 2013:55, 392-402.

[24] L. Zhao, W.J. Cai, X. d. Ding, W. c. Chang, Decentralized optimization for vapor compression refrigeration cycle, Applied Thermal Engineering, 2013:51, 753-763

[25] Zhang, L., Li, C., Li, Y. et al. Simultaneous optimization of multi parameters on a subcritical organic Rankine cycle system for low-grade waste heat recovery. J Mech Sci Technol 33, 447–458 (2019).

[26] Moghimi, M., Emadi, M., Ahmadi, P., & Moghadasi, H. (2018). 4E analysis and multi-objective optimization of a CCHP cycle based on gas turbine and ejector refrigeration. Applied Thermal Engineering, 141, 516-530.

[27] Khademi, M., Behzadi Forough, A., & Khosravi, A. (2019). Techno-economic operation optimization of an HRSG in combined cycle power plants based on evolutionary algorithms: A case study of Yazd, Iran. Energy Equipment and Systems, 7(1), 67-79.

[28] Hajabdollahi, H., & Esmaieli, A. (2017). Selection of the optimum prime mover and the working fluid in a regenerative organic Rankine cycle. Energy Equipment and Systems, 5(4), 325-339.

[29] Salim, M. S., & Kim, M. H. (2019). Multi-objective thermo-economic optimization of a combined organic Rankine cycle and vapour compression refrigeration cycle. Energy Conversion and Management, 199, 112054.

[30] Petrovic, A., Delibasic, B., Filipovic, J., Petrovic, A., & Lomovic, M. (2018). Thermoeconomic and environmental optimization of a geothermal water desalination plant with the ejector refrigeration system. Energy Conversion and Management, 178, 65-77.

[31] H. Abed, K. Atashkari, A. Niazmehr, A. Jamali, Thermodynamic optimization of combined power and refrigeration cycle using binary organic working fluid, International Journal of Refrigeration, 2013:36, 2160-2168.

[32] Kaşka, Ö., Yılmaz, C., Bor, O., & Tokgöz, N. (2018). The performance assessment of a combined organic Rankine-vapor compression refrigeration cycle aided hydrogen liquefaction. International Journal of Hydrogen Energy, 43(44), 20192-20202

[33] Ma, Y., Liu, M., Yan, J., & Liu, J. (2018). Performance investigation of a novel closed Brayton cycle using supercritical CO2-based mixture as working fluid integrated with a LiBr absorption chiller. Applied Thermal Engineering, 141, 531-547.

[34] Farzaneh. Hajabdollahi, Zahra. Hajabdollahi, Hassan. Hajabdollahi. Soft computing-based Multi-objective optimization of steam cycle power plant using NSGA-II and ANN. Applied Soft Computing 2012: 123648-3655.

[35] Sayyaadi H, Amlashi EH, Amidpour M. Multi-objective optimization of a vertical ground source heat pump using an evolutionary algorithm. Energy Convers Manage 2009; 50:2035-46.

[36] Hajabdollahi, H., Ahmadi, P., & Dincer, I. (2011). Multi-objective optimization of plain fin-and-tube heat exchanger using an evolutionary algorithm. Journal of thermophysics and heat transfer, 25(3), 424-431.

[37] K. Deb, T. Goel. Controlled elitist non-dominated sorting genetic algorithms for better convergence. In: Proceedings of the first international conference on evolutionary multi-criterion optimization, Zurich; 2001. p. 385–99

[38] K. Deb. Multi-objective optimization using evolutionary algorithms. Chichester: John Wiley and Sons Ltd, 2001.

[39] Hajabdollahi, Z., Hajabdollahi, F., Tehrani, M. and Hajabdollahi, H. "Thermo-economic environmental optimization of Organic Rankine Cycle for diesel waste heat recovery." Energy 63 2013: 142-151.